Supplementary Information

Control of Framework Interpenetration for *in situ* Modified Hydroxyl Functionalised IRMOFs

Damien Rankine,[a] Antonio Avanelleda,[a] Matthew R. Hill,[b] Christian J. Doonan,[a*] and Christopher J. Sumby[a*]

[a] *School of Chemistry & Physics, The University of Adelaide, Adelaide, Australia. CJD: Phone +61 8 8303 5770. Fax. +61 8 8303 4358. Email: christian.doonan@adelaide.edu.au; CJS: Phone +61 8 8303 7406. Fax. +61 8 8303 4358. Email: christopher.sumby@adelaide.edu.au*
[b] *CSIRO Materials Science and Engineering – Clayton, Clayton VIC 3168, Australia*

CONTENTS

LIST OF FIGURES AND TABLES

1. General Experimental

N,N'-Dimethylformamide (DMF) was dried twice consecutively over freshly activated 4 Å molecular sieves and stored under N_2 atmosphere. *N,N'*-Diethylformamide (DEF) was stirred over charcoal overnight, filtered through a plug of Celite and stored over activated 4 Å molecular sieves. ^{1}H and ^{13}C NMR spectra were recorded on a Varian Gemini spectrometer operating at 300 MHz and 75.1 MHz, respectively. ^{1}H and ^{13}C Spectra were referenced to 7.26 ppm and 77.0 ppm in $CDCl_3$ and 2.50 ppm and 39.6 ppm in d^6-DMSO, respectively. Melting points were recorded on a Reichert electrothermal melting point apparatus and are uncorrected. The Campbell microanalytical laboratory at the University of Otago, Dunedin performed all elemental analyses. Electrospray Ionisation-Mass Spectrometry (ESI-MS) was performed on a Finnigan LCQ mass spectrometer. Thermogravimetric analysis was performed on a Perkin−Elmer STA-6000 under a constant flow of N_2 at a temperature increase rate of 5°C/min. Infrared (IR) spectra were recorded on a Perkin−Elmer Fourier−Transform Infrared (FT−IR) spectrometer on a zinc−selenide crystal. N_2 adsorption isotherms at 77 K were recorded on a Micromeritics ASAP 2020 adsorption analyser. The Braunner-Emmett-Teller (BET) method[1] was used for determining surface areas from N_2 isotherms at 77 K and further validated using the method of Walton and Snurr.[2] CO_2 enthalpy plots were obtained with the use of Van't Hoff plots derived from isotherms collected at 273 and 298 K respectively on an ASAP 2420 gas adsorption analyser. Energy Dispersive Spectroscopy (EDS) was performed on a Philips XL30 Field Emission Scanning Electron Microscope (FESEM) at 10keV and further analysed using the program EDAX Genesis. Samples surfaces were coated in carbon prior to EDS analysis to reduce surface charging and improve resolution.

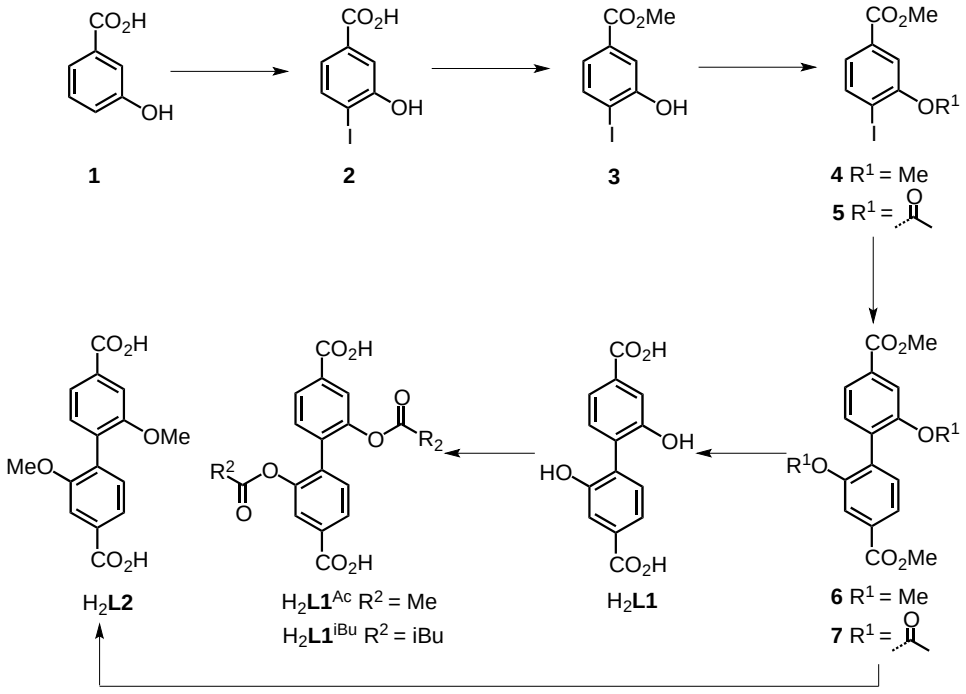

Scheme 1. Synthesis of H_2**L1**^{Ac}, H_2**L1**^{iBu} and H_2**L2**.

2. Synthetic Procedures

*4-Iodo-3-hydroxybenzoic acid (**2**)*

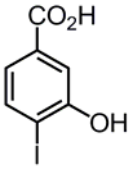

To a solution of 3-hydroxybenzoic acid (25.0 g, 181 mmol) in MeOH (250 mL), NaOH (7.51 g, 188 mmol) and NaI (28.17 g, 188 mmol) were added and stirred until dissolved. The solution was cooled to -10°C and 12.5% NaOCl solution (112 mL) was added dropwise over 1 hour such that the temperature did not exceed 3°C. The resulting dark red/orange solution was stirred for 1 hour at 0°C then at room temperature overnight to give a pale yellow suspension. The solvent was evaporated under reduced pressure, water was added (150 mL) and the solution acidified to pH 1 with concentrated HCl. The precipitate was collected by filtration under reduced pressure, and washed with water. The solid was recrystallised from 5:1 water/ethanol and dried in an oven at 80°C to give an off-white solid of 4-iodo-3-hydroxybenzoic acid (**2**) (27.8 g, 60%); M.p. 218-220°C; ^{1}H NMR (d^{6}-DMSO, 200 MHz): δ 10.68 (br. s, 1H), 7.79 (d, J = 8.0 Hz, 1H), 7.42 (d, J = 1.8 Hz, 1H), 7.12 (dd, J = 1.8, 8.0 Hz, 1H); ^{13}C NMR (d^{6}-DMSO, 50 MHz): δ 166.78, 156.70, 138.97, 132.08, 121.45, 114.99, 90.71.

*Methyl 4-iodo-3-hydroxybenzoate (**3**)*

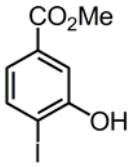

To a solution of 4-iodo-3-hydroxybenzoic acid (**2**) (25.9 g, 98 mmol) in MeOH (300 mL) was added concentrated H_2SO_4 (8.60 mL) and the solution heated at reflux overnight. The solution was cooled to 0°C and brought to pH 7 with saturated aqueous $NaHCO_3$ solution. The solvents were removed under reduced pressure, water was added and the solution extracted with EtOAc (3 x 60 mL). The combined organic extracts were washed with brine (80 mL), dried over anhydrous Na_2SO_4, filtered and evaporated under reduced pressure to give a colourless solid of methyl 4-iodo-3-hydroxybenzoate (**3**) (26.0 g, 95%); M.p. 168-172°C; ^{1}H NMR ($CDCl_3$, 200MHz): δ 7.75 (d, J = 8.2 Hz, 1H), 7.63 (d, J = 2.0 Hz, 1H), 7.33 (dd, J = 2.0, 8.2 Hz, 1H), 3.91 (s, 3H).^{13}C NMR ($CDCl_3$, 50 MHz): δ 166.66, 155.34, 138.80, 132.39, 123.20, 115.98, 91.88, 52.64.

*Methyl 4-iodo-3-methoxybenzoate (**4**)*

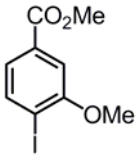

To a solution of methyl 4-iodo-3-hydroxybenzoate (**3**) (28.5 g, 102 mmol) and K_2CO_3 (17.3 g, 125 mmol) in acetone (170 mL) was added Me_2SO_4 (11.46 mL, 121 mmol) dropwise, and then heated at reflux for 4 hours under N_2 atmosphere. Water (70 mL) was added and the acetone evaporated under reduced pressure. The product was then extracted with CH_2Cl_2 (3 x 70 mL), dried over $MgSO_4$, filtered and evaporated under reduced pressure to a yellow oil, which solidified upon standing to give a hard, colourless solid methyl 4-iodo-3-methoxybenzoate (**4**) (29.5 g, 99%); M.p. 50-52°C (lit. M.p. 49°C)[1]; ^{1}H NMR ($CDCl_3$, 200 MHz): δ 7.85 (d, J = 8.2 Hz, 1H), 7.45 (d, J = 1.6 Hz, 1H), 7.37 (dd, J = 8.0, 1.6 Hz, 1H), 3.94 (s, 3H), 3.82 (s, 3H); ^{13}C NMR ($CDCl_3$, 50 MHz): δ 166.76, 158.53, 139.77, 131.94, 123.57, 111.52, 92.87, 56.74, 52.50.

*Methyl 4-iodo-3-acetoxybenzoate (**5**)*

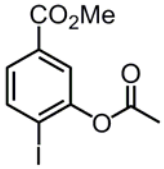

Concentrated H_2SO_4 (1.1 mL) was added to methyl 4-iodo-3-hydroxybenzoate (**4**) (26.0 g, 93.5 mmol) in acetic anhydride (30 mL) and was stirred at 80°C overnight. After cooling to room temperature, water (150 mL) was added and the solution extracted with $CHCl_3$ (3 x 50 mL). The combined organic extracts were passed through a plug of silica and washed with saturated $NaHCO_3$ solution, dried over $MgSO_4$, filtered and the solvents removed *in vacuo* to give a white solid of methyl 4-iodo-3-acetoxybenzoate (**5**) (27.2 g, 91%); M.p. 89-90°C; ^{1}H NMR ($CDCl_3$, 200MHz): δ 7.92 (d, J = 8.2 Hz, 1H), 7.73 (d, J = 1.8 Hz, 1H), 7.62 (dd, J = 8.2, 1.8 Hz, 1H), 3.91(s, 3H), 2.38 (s, 3H); ^{13}C NMR ($CDCl_3$, 50 MHz): δ 168.46, 165.89, 151.69, 139.83, 132.14, 128.44, 124.09, 97.29, 52.62, 21.32.

*Dimethyl 2,2'-dimethoxy-1,1'-biphenyl-4,4'-dicarboxylate (**6**)*

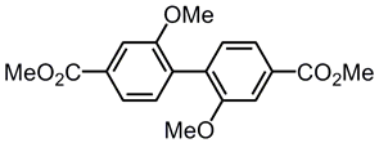

Prepared using a modified literature procedure:[3] Methyl 4-iodo-3-methoxybenzoate (**4**) (40.0 g, 136.9 mmol) was thoroughly mixed with activated copper bronze (50.0 g) and dried in *vacuo* with sonication, before heating at 210°C for 4 hours, under an Ar atmosphere. The solid residue was extracted with boiling ethyl acetate (1.5 L) and hot filtered to give a yellow solution. The solvent was then evaporated under reduced pressure and the remaining residue recrystallised from methanol and hot filtered to give dimethyl 2,2'-dimethoxy-1,1'-biphenyl-4,4'-dicarboxylate (**6**) as colourless blades (17.6 g, 78%); M.p. 167-169°C (lit. M.p. 165-166°C)[1]; IR (cm^{-1}): 2961(s), 2835(s), 1713, 1604, 1558, 1466, 1391, 1290; ^{1}H NMR ($CDCl_3$, 200MHz): δ 7.70 (dd, J = 1.6, 7.7 Hz, 2H), 7.64 (d, J = 1.6 Hz, 2H), 7.3 (d, J = 7.7 Hz, 2H), 3.94 (s, 6H), 3.82 (s, 6H); ^{13}C NMR ($CDCl_3$, 50 MHz): δ 166.91, 156.95, 131.86, 131.13, 130.95, 121.79, 111.95, 55.87, 52.14; ES-MS: *m/z* 314.9 [M-CH_3]$^-$.

*Dimethyl 2,2'-bis(acetoxy)-1,1'-biphenyl-4,4'-dicarboxylic acid (**9**)*

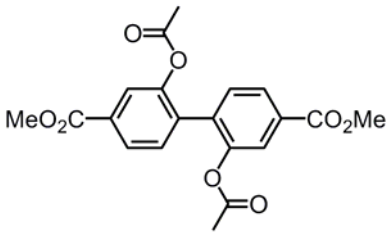

Methyl 4-iodo-3-acetoxybenzoate (**5**) (28.0 g, 87.4 mmol) and activated copper bronze (35.0 g) were thoroughly mixed, with sonication, and heated at 210°C under Ar atmosphere for 5 hours. The mixture was extracted with hot EtOAc, filtered and the solvent removed under reduced pressure. The residue was dry loaded onto a column of silica gel and purified by dry flash chromatography (10:1 to 4:1 Hexane/EtOAc). The pure fractions were combined to give a colourless solid dimethyl 2,2'-bis(acetoxy)-1,1'-biphenyl-4,4'-dicarboxylic acid (**7**) as a white solid (7.6 g, 45%); M.p. 117-118°C; ^{1}H NMR ($CDCl_3$, 200MHz): δ 7.98 (dd, J = 8.0, 1.6 Hz, 2H), 7.86 (d, J = 1.6 Hz, 2H), 7.39 (d, J = 8.0 Hz, 2H), 3.94(s, 6H), 2.06 (s, 6H);^{13}C NMR ($CDCl_3$, 50 MHz): δ 169.00, 166.09, 148.20, 134.69, 131.83, 131.31, 127.29, 124.27, 52.58, 20.79.

*2,2'-Dihydroxy-1,1'-biphenyl-4,4'-dicarboxylic acid (H_2**L1**)*

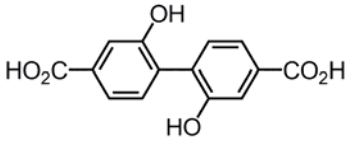

Method 1: To a solution of dimethyl 2,2'-dimethoxy-1,1'-biphenyl-4,4'-dicarboxylate (**6**) (3.42 g, 10.3 mmol) in dry CH_2Cl_2 (95 mL) at -78°C, was added a solution of BBr_3 (3.92 ml, 41.5 mmol) in dry CH_2Cl_2 (26 mL), dropwise over several minutes, under Ar atmosphere. The resulting orange solution was stirred at -78°C for 30 mins and slowly warmed to room temperature overnight, with stirring. The yellow suspension was stirred at room temperature for a further 24 hours. The solution was poured onto ice-cold water, neutralised with 2M NaOH solution and then re-acidified to pH 6 with conc. HCl solution. The resulting suspension was repeatedly extracted with ethyl acetate (6 x 80 mL) and the combined organic extracts washed with water (80 mL) and brine (80 mL), dried over $MgSO_4$ and filtered. The solvent was evaporated under reduced pressure and dried *in vacuo* to give a colourless solid 2,2'-dihydroxy-1,1'-biphenyl-4,4'-dicarboxylic acid (H_2**L1**) (2.2 g, 79%).

Method 2: Dimethyl 2,2'-bis(acetoxy)-1,1'-biphenyl-4,4'-carboxylic acid (**7**) (5.9 g, 15.3 mmol) was added to a solution of NaOH (9.55 g, 238 mmol) in H_2O (120 mL), MeOH (25 mL) and THF (250 mL) and stirred at room temperature overnight. After cooling, the solvents were evaporated to give an orange solution to which was added further water (100 mL) and the solution acidified to pH 1 with concentrated aqueous HCl. The solution was cooled to 0°C and filtered, washing with cold water. The solid was then dried at 80°C for 2 hours to give a colourless solid 2,2'-dihydroxy-1,1'-biphenyl-4,4'-dicarboxylic acid (H_2**L1**) (4.10 g, 98%). M.p. >360°C (decomp.);^{1}H NMR (d^6-DMSO, 200MHz): δ 12.80 (br. s, 2H), 9.75 (br. s, 2H), 7.50 (d, J = 1.4 Hz, 2H), 7.41 (dd, J = 1.6, 7.8 Hz, 2H), 7.26 (d, J = 7.8 Hz, 2H); ^{13}C NMR (d^6-DMSO, 50 MHz): δ 167.13, 154.53, 131.28, 130.88, 119.57, 116.26, 82.01.

*2,2'-Bis(acetoxy)-1,1'-biphenyl-4,4'-dicarboxylic acid (H_2**L1**^{Ac})*

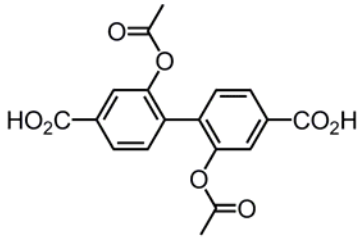

To a suspension of 2,2'-dihydroxy-1,1'-biphenyl-4,4'-dicarboxylic acid (H_2**L1**) (0.50 g, 1.82 mmol) in Ac_2O (2.0 mL) was added concentrated H_2SO_4 (2 drops). The resulting solution was heated at 70°C for 1 hour and then cooled to 2-3°C. Water (10 mL) was added and the precipitate was collected by filtration under reduced pressure and further washed with water. The filtrate was cooled to 2-3°C and filtered again to yield a second crop of material. The combined residue was recrystallised from EtOH and dried by azeotropic distillation (toluene) to give a colourless solid 2,2'-bis(acetyloxy)-1,1'-biphenyl-4,4'-dicarboxylic acid (H_2**L1**^{Ac}) (0.56 g, 86%). M.p. 245-248°C; Analysis calc. for $C_{18}H_{14}O_8$ C 60.33, H 3.95; found C 60.09, H 3.92; IR (cm^{-1}): 3099-2989, 2656, 2543, 1773, 1763, 1687, 1426, 1179; ^{1}H NMR (d^6-DMSO, 200MHz): δ 13.25 (br. s, 2H), 7.91 (dd, J = 1.4, 7.9 Hz, 2H), 7.81 (d, 1.6 Hz, 2H), 7.43 (d, J = 7.8 Hz, 2H), 2.04 (s, 6H); ^{13}C NMR (d^6-DMSO, 50 MHz): δ 168.59, 166.14, 147.53, 133.46, 132.04, 131.09, 126.60, 123.72, 20.32. ES-MS: *m/z* 356.9 $(M\text{-}H^+)^-$.

*2,2'-Bis(isobutyloxy)-1,1'-biphenyl-4,4'-dicarboxylic acid (H_2**L1**^{iBu})*

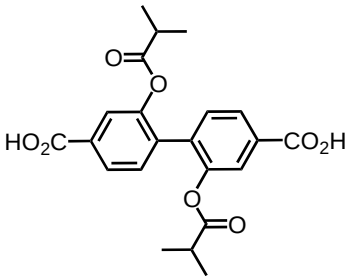

A suspended solution of 2,2'-dihydroxy-1,1'-biphenyl-4,4'-dicarboxylic acid (H_2**L1**) (150 mg, 0.54 mmol) in isobutyric anhydride (1.0 mL) was heated to 70°C and concentrated H_2SO_4 (3 drops) was added, giving a clear yellow solution, which was stirred at 70°C for 2 hours, cooled to room temperature and quenched with water. The precipitate was collected by filtration under reduced pressure, washing with water, and dried by azeotropic distillation (toluene) to give a colourless solid of 2,2'-bis(butyloxy)-1,1'-biphenyl-4,4'-dicarboxylic acid (H_2**L1**^{iBu}) (137 mg, 58%); M.p. 228-233°C, IR (cm^{-1}): 2985, 2945, 2551, 1766, 1689, 1608, 1562, 1415, 1290, 1119; ^{1}H NMR (d^6-DMSO, 300MHz): δ 12.78 (br. s, 2H), 7.90 (d, J = 8.0 Hz, 2H), 7.79 (s, 2H), 7.43 (dd, J = 0.8, 8.0 Hz, 2H), 2.32 (t, J = 7.4 Hz, 2H), 0.93 (s, J = 7.4Hz, 12H); ^{13}C NMR (d^6-DMSO, 50 MHz): δ 166.15, 147.58, 133.52, 132.03, 131.03, 126.51, 123.59, 82.05, 26.61, 8.45.

*2,2'-Dimethoxy-1,1'-biphenyl-4,4'-dicarboxylic acid (H_2**L2**)*

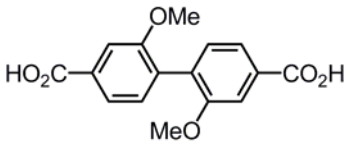

Dimethyl 2,2'-dimethoxy-1,1'-biphenyl-4,4'-dicarboxylate (**8**) (0.65 g, 1.97 mmol) in a mixture of 2M NaOH solution (15 mL), MeOH (4 mL) and THF (40 mL) and was stirred at room temperature overnight. THF and methanol were evaporated under reduced pressure and the remaining solution acidified to pH 1 with concentrated HCl solution. The white suspension was cooled over ice and the solid was collected by filtration, washing with water and the dried by azeotropic distillation (toluene) to give a colourless solid of 2,2'-dimethoxy-1,1'-biphenyl-4,4'-dicarboxylic acid (H_2**L2**) (0.54 g, 91%); M.p. 309-312°C; IR (cm^{-1}): 2945 (br), 2648 (br), 1679, 1568, 1416, 1286; ^{1}H NMR (d^6-DMSO, 200MHz): δ 7.61-7.56 (m, 4H), 7.28 (d, J = 8 Hz, 2H), 3.76 (s, 6H); ^{13}C NMR (d^6-DMSO, 50 MHz): δ 166.98, 156.56, 131.60, 131.09, 130.91, 121.29, 111.60, 55.59; ES-MS: *m/z* 300.9 $(M-H^+)^-$.

Preparation of Activated Copper Bronze

Copper bronze (5.0 g) was stirred in an aqueous solution of 20mM Na_2EDTA (50 mL) for 2 hours. The supernatant was decanted and the solid was washed with degassed H_2O (2 x 70 mL) and degassed MeOH (2 x 70 mL), collected by filtration under reduced pressure and dried *in vacuo* to give a salmon-coloured solid of activated copper bronze, which was used immediately or alternatively, stored in a dessicator until further use.

3. MOF Synthesis and Activation

Synthesis:

*Synthesis of [Zn_4O(**L1**)$_3$]*

H_2**L1**^{Ac} **or** H_2**L1**^{iBu} (30 mg) and $Zn(NO_3)_2.6H_2O$ (4.0 mol eq.) were dissolved in *N,N'*-diethylformamide (DEF) (4.5 mL). To this was added 2.5 M aqueous NaOH (30 µL) and the solution heated at 90°C for 20 mins in a capped 20 mL glass vial. The solution was then decanted into a fresh vial and heated at 90°C for 36 hours yielding colourless cubic crystals of [Zn_4O(**L1**)$_3$] (Yield: 60-70% after activation - based on ligand). Analysis calc. for [$Zn_4O(C_{14}H_8O_6)_3$]·DEF: C 47.22 H 2.96 ; found C 47.55, H 2.84.

*Synthesis of α-[Zn_4O(**L1**)$_3$]*

H_2**L1**^{Ac} **or** H_2**L1**^{iBu} (30 mg) and $Zn(NO_3)_2.6H_2O$ (4.0 mol eq.) were dissolved in *N,N'*-dimethylformamide (DMF) (4.5 mL). To this was added 2.5 M aqueous NaOH (30 µL) and the solution heated at 90°C for 20 mins in a capped 20 mL glass vial. The solution was then decanted into a fresh vial and heated at 90°C for a further 36 hours yielding colourless cubic crystals of α-[Zn_4O(**L1**)$_3$] (Yield: 60-70% after activation - based on ligand). Analysis calc. for [$Zn_4O(C_{14}H_8O_6)_3$]·DMF: C 46.30, H 2.68; found C 46.70, H 2.90.

*Synthesis of [Zn_4O(**L1**^{Ac})$_3$]*

H_2**L1**^{Ac} (30 mg) and $Zn(NO_3)_2.6H_2O$ (4.0 mol eq.) were dissolved in *N,N'*-diethylformamide (DEF) (4.5 mL) and the solution heated to 90°C for 24 hours yielding colourless cubic crystals of [Zn_4O(**L1**^{Ac})$_3$] (Yield: 76% after activation - based on ligand). Analysis calc. for [$Zn_4O(C_{18}H_{12}O_8)_3$]·DEF: C 48.95, H 3.28; found C 48.59, H 3.40.

*Synthesis of α-[Zn_4O(**L1**^{Ac})$_3$]*

H_2**L1**^{Ac} (30 mg) and $Zn(NO_3)_2.6H_2O$ (4.0 mol eq.) were dissolved in *N,N'*-dimethylformamide (DMF) (4.5 mL) and the solution heated to 90°C for 24 hours yielding colourless cubic crystals of α-[Zn_4O(**L1**^{Ac})$_3$] (Yield: 78% after activation - based on ligand). Analysis calc. for [$Zn_4O(C_{18}H_{12}O_8)_3$]: C 48.17, H 2.70; found C 48.06, H 3.21.

*Synthesis of α-[Zn_4O(**L2**)$_3$]*

H_2**L2** (30 mg) and $Zn(NO_3)_2.6H_2O$ (4.0 mol eq.) were dissolved in *N,N'*-diethylformamide (DEF) (4.5 mL) The solution was then heated at 90°C for 12 hours yielding colourless, cubic crystals of α-[Zn_4O(**L2**)$_3$] (Yield: 71% after activation – based on ligand). Analysis calc. for [$Zn_4O(C_{16}H_{12}O_6)_3$]: C 48.92, H 3.09; found C 48.88, H 3.41.

Activation:

*[Zn_4O(**L1**)$_3$], [Zn_4O(**L1**^{Ac})$_3$]*:

The crystals were washed with dry DMF five times over 2 hours and then soaked in dry DMF overnight. The crystals were then washed with dry acetone five times over 2 hours and soaked in dry acetone overnight. The fully acetone-exchanged material was then activated via solvent exchange with LCO_2 (1.5 hours) and solvent removal above the critical point of CO_2 (1 hour) on a Samdri-PVT-3D Critical-Point-Dryer.

*α-[Zn_4O(**L2**)$_3$], α-[Zn_4O(**L1**)$_3$], α-[Zn_4O(**L1**^{Ac})$_3$], α-[Zn_4O(**L1**^{iBu})$_3$]*: The crystals were activated by washing with dry DMF three times over 2 hours and then soaking in dry DMF overnight. Solvent exchange with dry CH_2Cl_2 occurred by washing the solution with dry CH_2Cl_2 three times over 2 hours and then soaking in dry CH_2Cl_2 overnight. Removal of solvent under reduced pressure at 80°C yielded the solvent-free, activated material.

4. MOF Characterisation

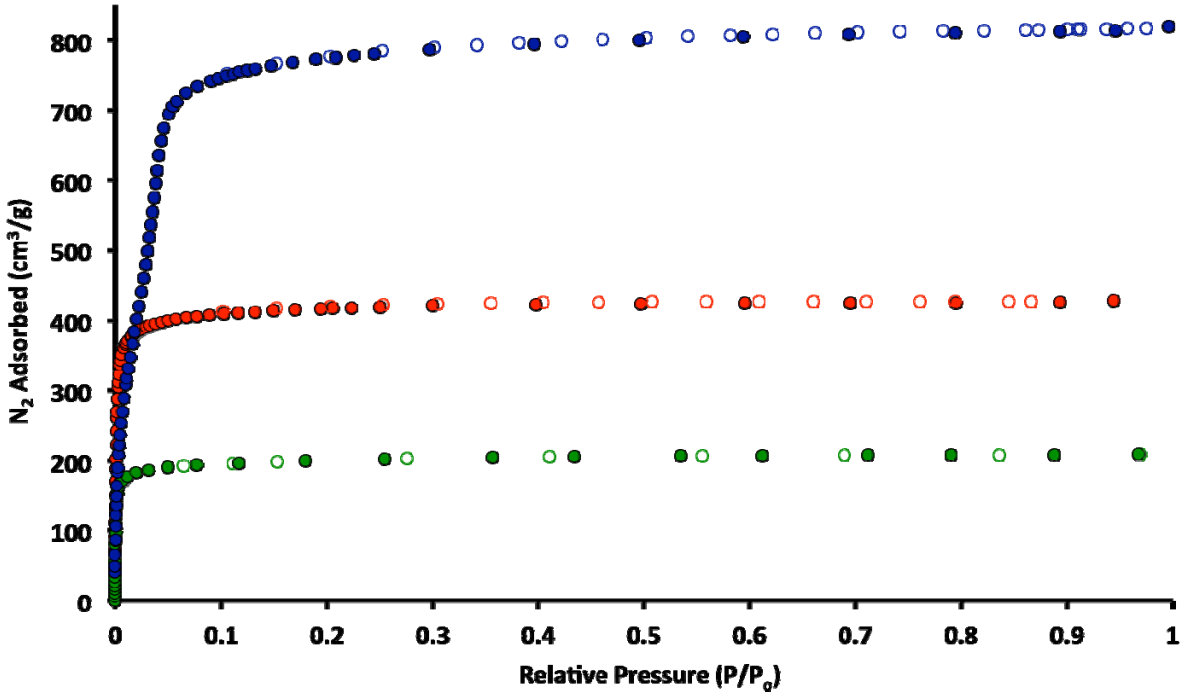

Figure S1. N_2 adsorption isotherms at 77 K of [Zn_4O(**L1**^{Ac})$_3$] (blue), α-[Zn_4O(**L2**)$_3$] (red), and α-[Zn_4O(**L1**^{iBu})$_3$] (green). Filled and open circles represent adsorption and desorption points respectively.

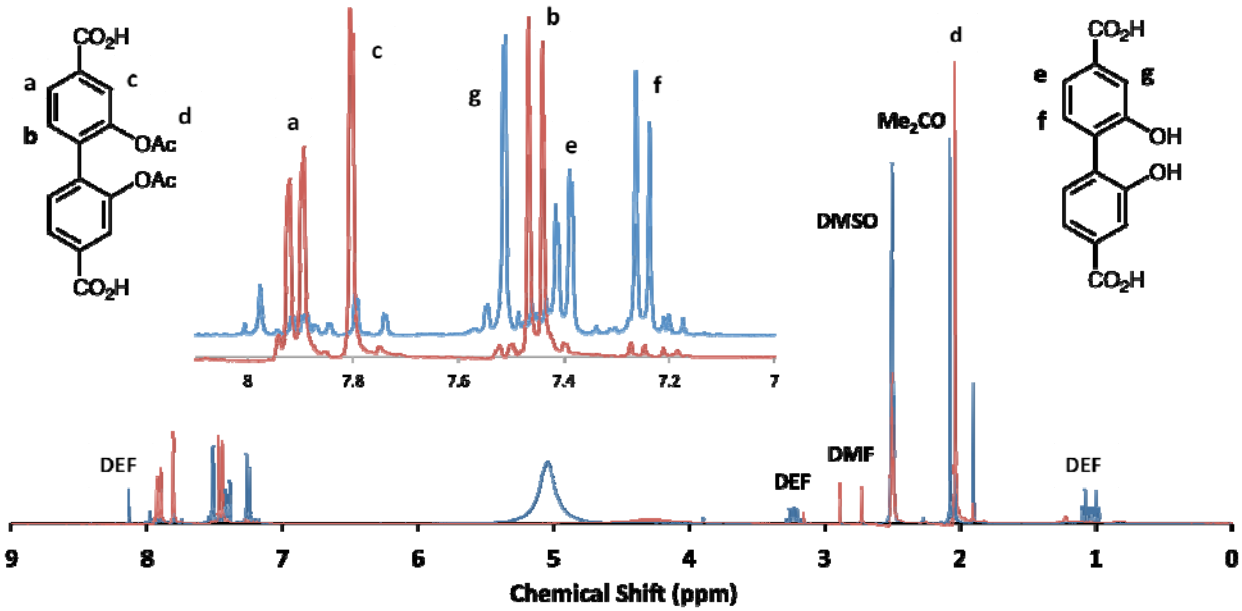

Figure S2. ^{1}H NMR (300 MHz) analysis of digested [Zn_4O(**L1**)$_3$] (blue) and α-[Zn_4O(**L1**^{Ac})$_3$] (red). Distinct changes in chemical shift of the aromatic hydrogen atoms allow for quick analysis of the extent of ester hydrolysis within the MOF.^

^10 mg samples of Metal-organic framework material were washed quickly with DMF, then acetone and dried under nitrogen for several minutes. The material was dissolved in d^6-DMSO (0.4 mL) and treated with 0.1 mL of stock solution of 35% DCl/D_2O (40μL) in d^6-DMSO (0.5 mL) and spectra were recorded immediately once the material had completely dissolved.

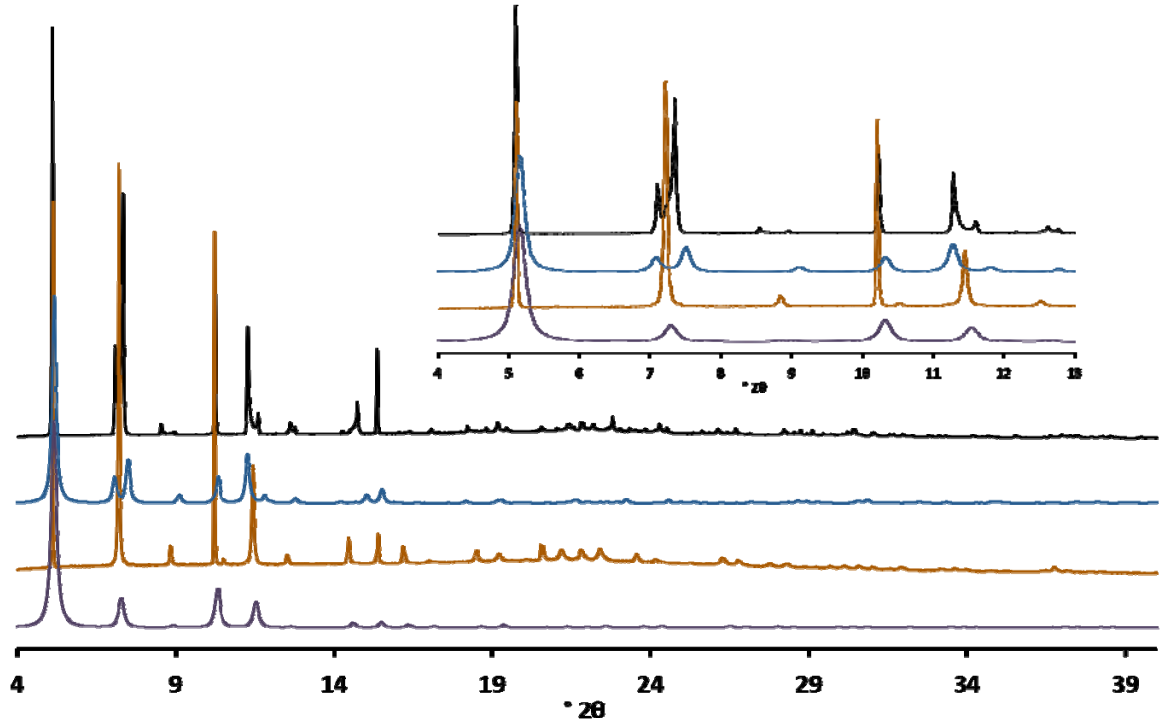

Figure S3. Experimental Powder X-Ray Diffraction (PXRD) patterns for $[Zn_4O(\mathbf{L1})_3]$ (brown) and α-$[Zn_4O(\mathbf{L1})_3]$ (black), and calculated PXRD patterns for $[Zn_4O(\mathbf{L1})_3]$ (purple) and α-$[Zn_4O(\mathbf{L1})_3]$ (blue). (**inset)** enlarged region in which peak splitting can be observed for interpenetrated frameworks.

Subtle differences between interpenetrated and non-interpenetrated structures are observed in the PXRD. For example, splitting of powder X-ray diffraction peaks around 2θ = 7.3 and 11.5° are observed for the interpenetrated frameworks relative to those which are non-interpenetrated and of higher symmetry. These additional peaks are characteristic of the various lower symmetry space groups adopted by the interpenetrated frameworks. In these frameworks, the peak positions, splitting and intensity vary slightly from sample to sample due to solvation and the nature of the packing of the two frameworks relative to each other.

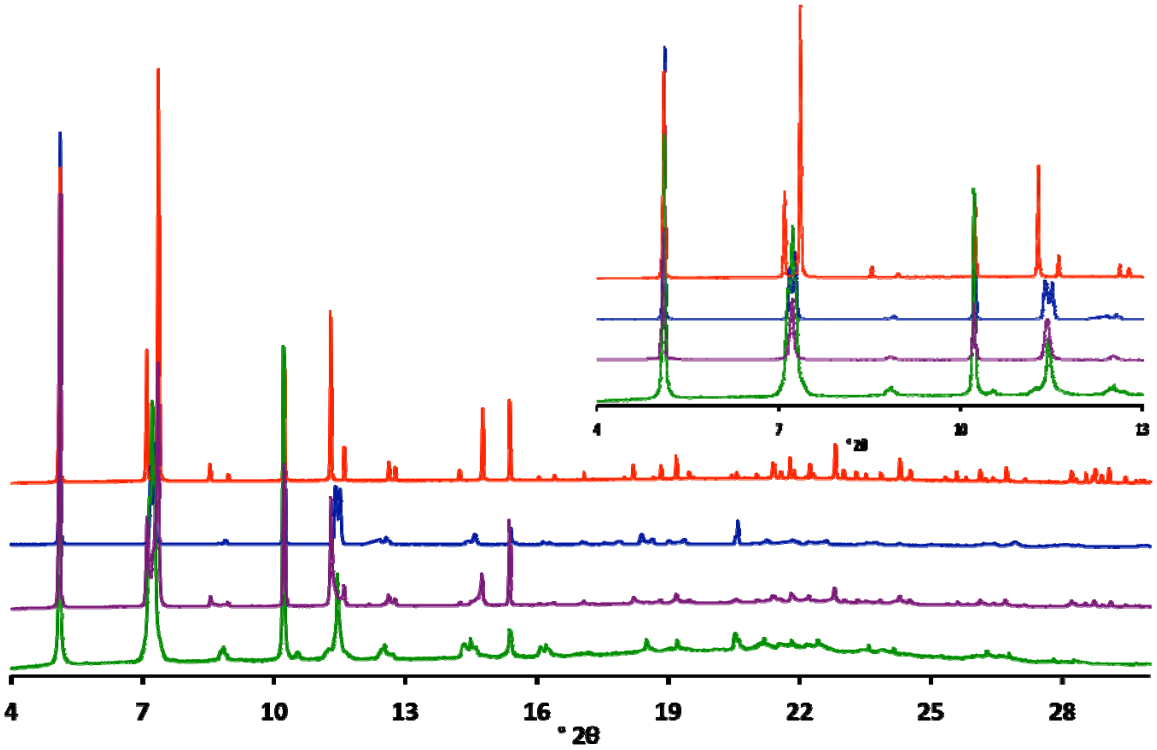

Figure S4. Powder X-Ray Diffraction (PXRD) patterns for $[Zn_4O(\mathbf{L1}^{Ac})_3]$ (green), α-$[Zn_4O(\mathbf{L1}^{Ac})_3]$ (purple), α-$[Zn_4O(\mathbf{L1}^{iBu})_3]$ (blue), α-$[Zn_4O(\mathbf{L2})_3]$ (red). **(inset)** enlarged region in which peak splitting can be observed for interpenetrated frameworks.

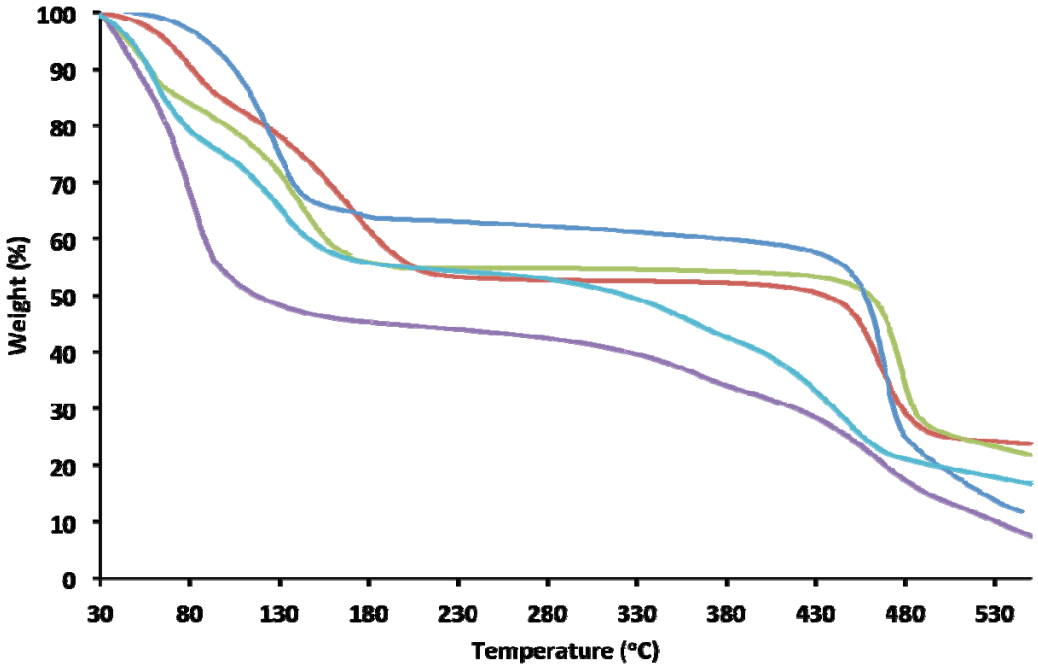

Figure S5. Thermogravimetric analysis of $[Zn_4O(\mathbf{L1})_3]$ (purple), $[Zn_4O(\mathbf{L1}^{Ac})_3]$ (light blue), α-$[Zn_4O(\mathbf{L1})_3]$ (red), α-$[Zn_4O(\mathbf{L1}^{iBu})_3]$ (green) and α-$[Zn_4O(\mathbf{L2})_3]$ (blue).

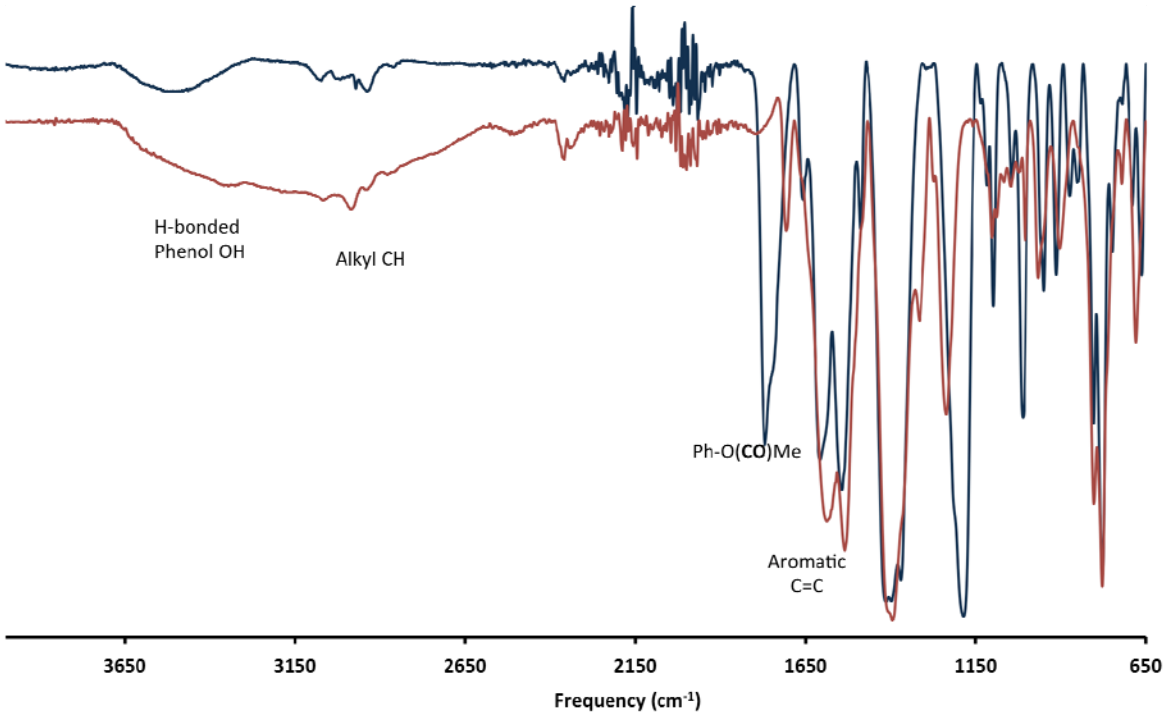

Figure S6. IR absorption spectra of $[Zn_4O(\mathbf{L1})_3]$ (red) and $[Zn_4O(\mathbf{L1}^{Ac})_3]$ (blue) showing the loss of the C=O vibrational frequency upon hydrolysis of the acetyl ester group yielding $[Zn_4O(\mathbf{L1})_3]$.

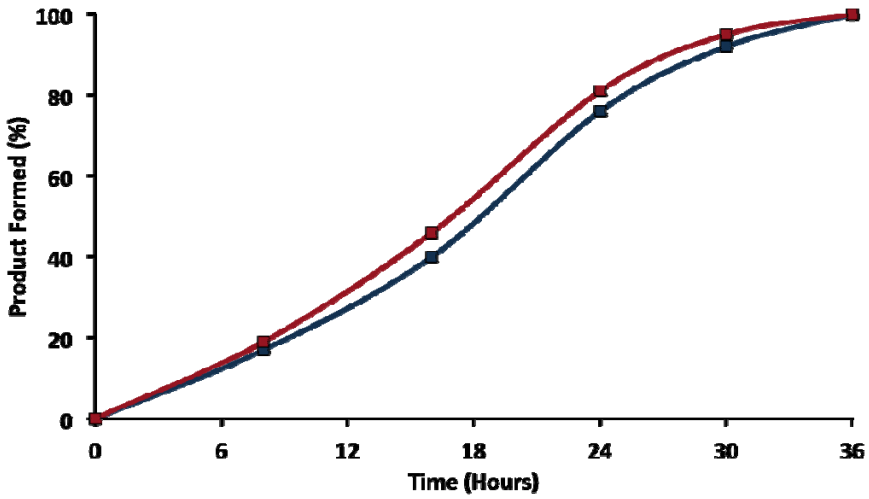

Figure S7. ^{1}H NMR digestion studies on the formation of $[Zn_4O(\mathbf{L1})_3]$ (red) and α-$[Zn_4O(\mathbf{L1})_3]$ (blue) in DEF and DMF, respectively. ^{1}H NMR spectra were completed immediately following washing and digestion.^

5. Metallation experiments for $[Zn_4O(L1)_3]$ and α-$[Zn_4O(L1)_3]$

A typical experiment involved the addition of a 0.05 M solution of $CuCl_2.2H_2O$ (1 mL) to $[Zn_4O(\mathbf{L1})_3]$ or α-$[Zn_4O(\mathbf{L1})_3]$ (30 mg) in DMF (1 mL) and left to stand at room temperature for 2 hours. The crystals typically begin to show a colour change within several minutes and become dark green in colour within 1-2 hours.

Activation:

Metallated samples of $[Zn_4O(\mathbf{L1})_3]$ or α-$[Zn_4O(\mathbf{L1})_3]$ were soaked in DMF (5 x 5 mL) over 5 hours to remove unreacted Cu(II). The washed samples were then soaked in dry acetone (5 x 5 mL) over 3 hours and then left to soak in acetone overnight. The fully acetone-exchanged material was then activated via solvent exchange with LCO_2 (1.5 hours) and solvent removal above the critical point of CO_2 (1 hour) on a Samdri-PVT-3D Critical-Point-Dryer.

6. Characterisation of $[Zn_4O(L1)_3]\supset Cu$ and α-$[Zn_4O(L1)_3]\supset Cu$

$[Zn_4O(L1)_3]\supset Cu$ and α-$[Zn_4O(L1)_3]\supset Cu$ were analysed by PXRD to determine their phase purity, TGA/DSC coupled to FTIR to identify the fragments released upon thermal treatment, and electron dispersive spectroscopy (EDS) to determine the Zn:Cu ratios in both $[Zn_4O(L1)_3]\supset Cu$ and α-$[Zn_4O(L1)_3]\supset Cu$.

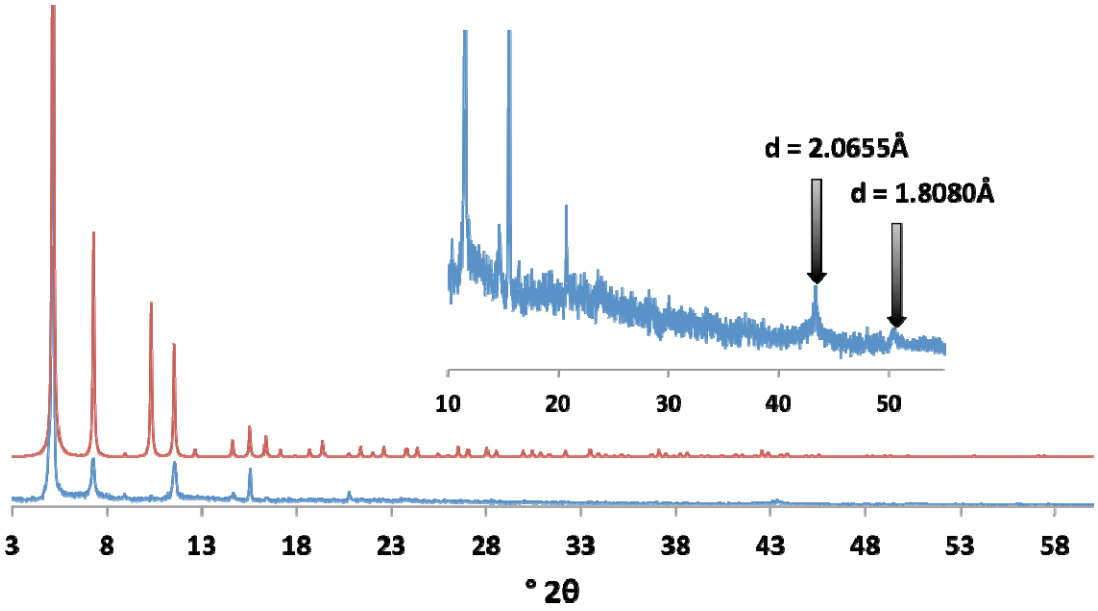

Figure S8. Calculated PXRD pattern from the crystal structure of $[Zn_4O(\mathbf{L1})_3]$ (red) and $[Zn_4O(\mathbf{L1})_3]\supset CuΔ$ (blue) that was heated to 300°C under a vacuum of 10 μbar for 2 hours. Inset: reflections corresponding to the formation of elemental Cu within the sample.

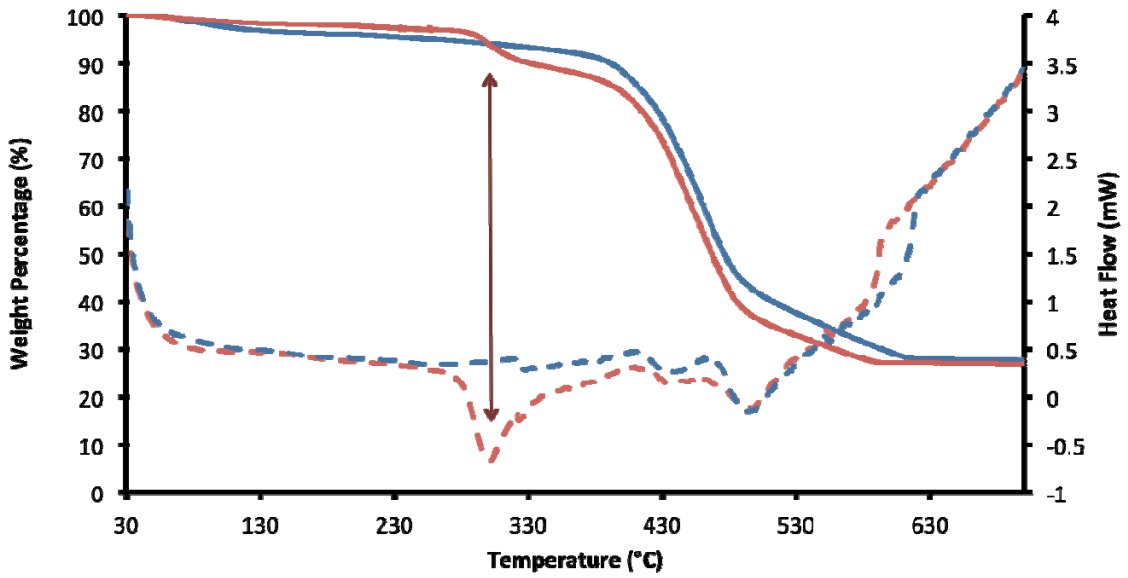

Figure S9. Thermogravimmetric analysis (TGA - line) and differential scanning calorimetry (DSC – dotted line) for α-$[Zn_4O(\mathbf{L1})_3]\supset Cu$. The loss of weight at approximately 300°C was probed by coupling the TGA-DSC measurements to FT-IR spectroscopy (Figure S8).

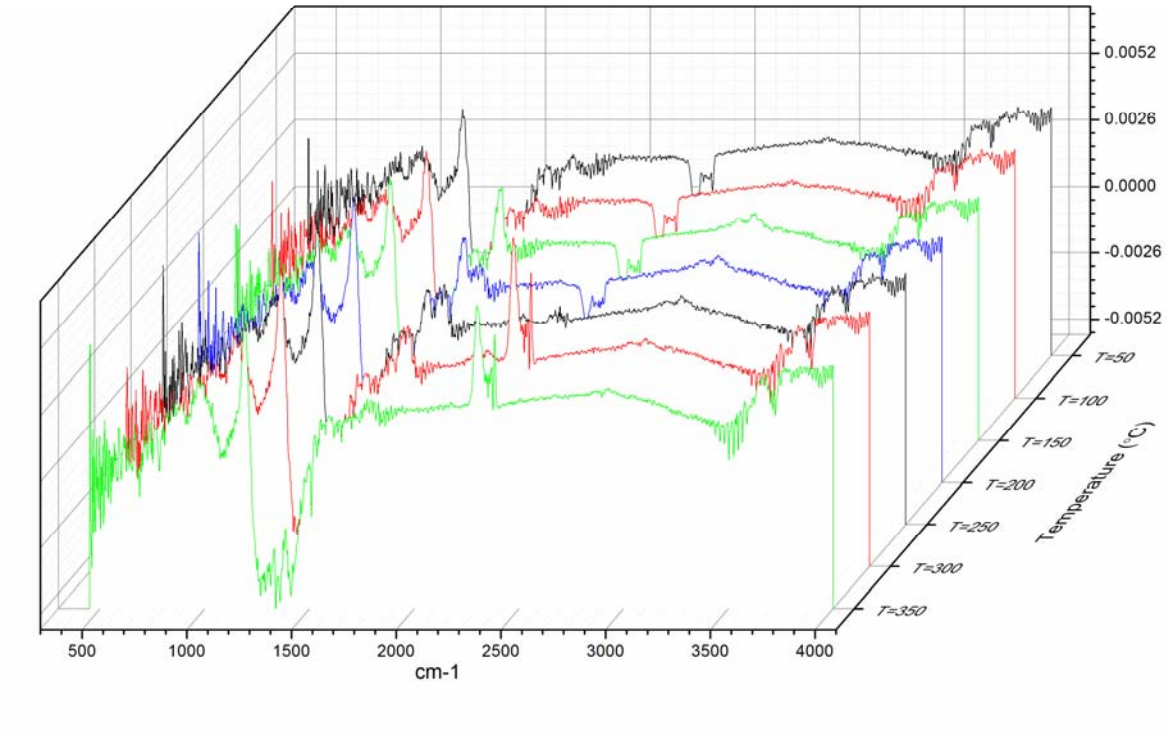

Figure S10. Gas-Phase FTIR spectra of α-$[Zn_4O(\mathbf{L1})_3]\supset Cu$ coupled to TGA-DSC (see Figure S8).

Permanent features of the spectra can be seen in the regions 700-450 and 1500-1200 cm^{-1}. The spectra of interest correlate to temperatures in the region 300-350°C on the TGA trace (Figure S9). Over this range we see a mass loss, not associated with framework decomposition, as well as a prominent endothermic change in the DSC. In the spectra recorded over this temperature range (300-350°C) the prominent CO_2 band around 2400-2300 cm^{-1} is observed and suggests the decomposition of coordinated DMF to CO_2 and dimethylamine. As we have not observed any absorption associated with the release of dimethylamine we can surmise that is not removed from the pores during this process. The weak carbonyl (C=O) absorption bands around 1700 cm^{-1} indicates that only small amounts of DMF is being released. Formic acid also absorbs around 1700 cm^{-1} yet no other distinctive absorption bands are seen that would indicate this. As expected water has been adsorbed from the air, due to some exposure related with sample transfer, which was shown to be removed up to a temperature of 200°C. This was evident from broad absorption bands at ~3500 cm^{-1},.

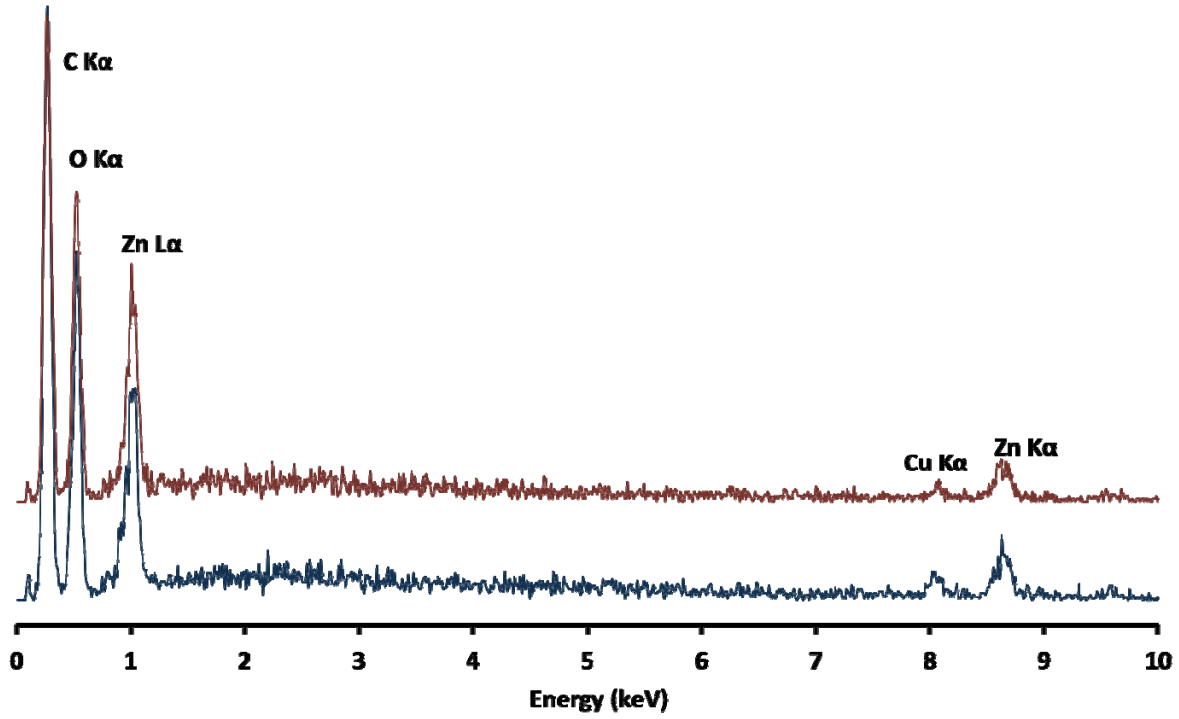

Figure S11. Illustrative EDS analyses of $[Zn_4O(\mathbf{L1})_3]\supset Cu$ **(red)** and α-$[Zn_4O(\mathbf{L1})_3]\supset Cu$ **(blue)** that provided averaged Zn:Cu ratios of 5:1 and 4:1, respectively.

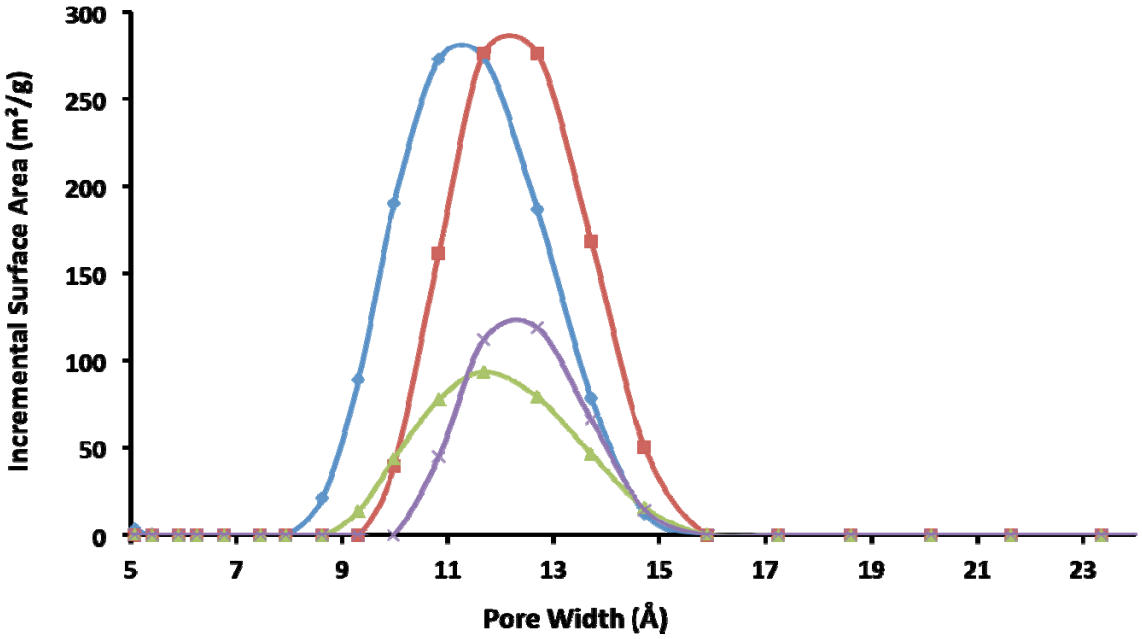

Figure S12. Pore Size Distribution of α-[Zn_4O(**L2**)$_3$] (red), α-[Zn_4O(**L1**)$_3$] (blue)**,** α-[Zn_4O(**L1**)$_3$]⊃Cu (green)**,** α-[Zn_4O(**L1**)$_3$]⊃CuΔ (purple) from Ar adsorption isotherms at 87 K.

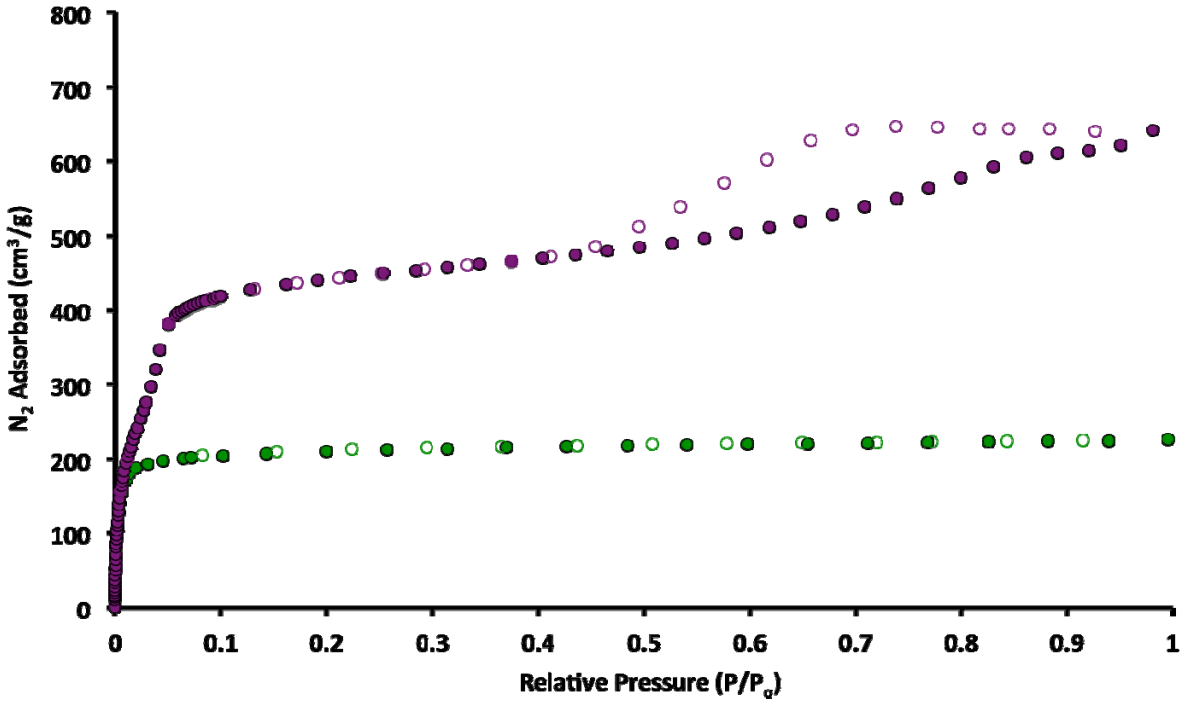

Figure S13. N_2 adsorption isotherms at 77 K of [Zn_4O(**L1**)$_3$]⊃Cu (purple) and α-[Zn_4O(**L1**)$_3$]⊃Cu (green).

7. BET Plot Data for $[Zn_4O(L1)_3]$, $[Zn_4O(L1^{Ac})_3]$, $[Zn_4O(L1)_3]\supset Cu$, α-$[Zn_4O(L1)_3]$, α-$[Zn_4O(L1^{iBu})_3]$, α-$[Zn_4O(L2)_3]$ and α-$[Zn_4O(L1)_3]\supset Cu$, respectively.

BET Surface Area:	2631.0518 ± 35.8195 m²/g
Slope:	0.001644 ± 0.000022 g/cm³ STP
Y-Intercept:	0.000011 ± 0.000001 g/cm³ STP
C:	156.253114
Qm:	604.3950 cm³/g STP
Correlation Coefficient:	0.9998129
Molecular Cross-Sectional Area:	0.1620 nm²

Relative Pressure (p/p°)	**Quantity Adsorbed (cm³/g STP)**
0.050119431	566.0127616
0.052486902	572.9000528
0.061936906	588.7007696
0.067230801	594.1288159

Table S1a. BET plot data for $[Zn_4O(\mathbf{L1})_3]$

BET Surface Area:	2833.3346 ± 96.6273 m²/g
Slope:	0.001516 ± 0.000052 g/cm³ STP
Y-Intercept:	0.000021 ± 0.000001 g/cm³ STP
C:	74.873748
Qm:	650.8627 cm³/g STP
Correlation Coefficient:	0.9982134
Molecular Cross-Sectional Area:	0.1620 nm²

Relative Pressure (p/p°)	**1/[Q(p°/p - 1)]**
0.016032639	4.44923E-05
0.01808263	4.80645E-05
0.020346926	5.17081E-05
0.022547738	5.49009E-05
0.024896292	5.7915E-05

Table S1b. BET plot data for $[Zn_4O(\mathbf{L1^{Ac}})_3]$

BET Surface Area:	1675.5751 ± 6.7818 m²/g
Slope:	0.002593 ± 0.000010 g/cm³ STP
Y-Intercept:	0.000005 ± 0.000001 g/cm³ STP
C:	551.181191
Qm:	384.9066 cm³/g STP
Correlation Coefficient:	0.9999428
Molecular Cross-Sectional Area:	0.1620 nm²

Relative Pressure (P/Po)	**Quantity Adsorbed (cm³/g STP)**
0.062410055	398.7225862
0.065056219	400.8591196
0.067677027	402.8196197
0.07029197	404.6484914
0.074035164	406.9557015
0.077753283	409.1190724
0.081489961	411.119664
0.085217567	412.8604321
0.092776325	416.0731546

Table S1c. BET plot data for $[Zn_4O(\mathbf{L1})_3]\supset Cu$

BET Surface Area:	1790.8699 ± 18.5267 m²/g
Slope:	0.002426 ± 0.000025 g/cm³ STP
Y-Intercept:	0.000004 ± 0.000000 g/cm³ STP
C:	561.161505
Qm:	411.3917 cm³/g STP
Correlation Coefficient:	0.9996780
Molecular Cross-Sectional Area:	0.1620 nm²

Relative Pressure (p/p°)	**Quantity Adsorbed (cm³/g STP)**
0.001909875	219.3595876
0.002437747	238.7153283
0.002930919	254.9114145
0.003600567	273.605172
0.004275832	289.5679678
0.005173605	307.2933639
0.006459388	325.8449936
0.007858631	339.7087482

Table S1d. BET plot data for α-$[Zn_4O(\mathbf{L1})_3]$

BET Surface Area:	795.2531 ± 1.7907 m²/g
Slope:	0.005472 ± 0.000012 g/cm³ STP
Y-Intercept:	0.000002 ± 0.000000 g/cm³ STP
C:	2488.080945
Qm:	182.6825 cm³/g STP
Correlation Coefficient:	0.9999848
Molecular Cross-Sectional Area:	0.1620 nm²

Relative Pressure (P/Po)	**1/[Q(Po/P - 1)]**
0.001225204	8.43387E-06
0.001891295	1.22756E-05
0.002854071	1.77616E-05
0.004581767	2.74763E-05
0.006584943	3.85842E-05
0.011368797	6.48169E-05
0.019675326	0.000109971
0.031561208	0.000174615

Table S1e. BET plot data for α-[Zn_4O(**L1**^{iBu})$_3$]

BET Surface Area:	1704.1929 ± 0.4277 m²/g
Slope:	0.002552 ± 0.000001 g/cm³ STP
Y-Intercept:	0.000002 ± 0.000000 g/cm³ STP
C:	1327.015475
Qm:	391.4806 cm³/g STP
Correlation Coefficient:	0.9999999
Molecular Cross-Sectional Area:	0.1620 nm²

Relative Pressure (p/p°)	**Quantity Adsorbed (cm³/g STP)**
0.002862604	310.9482548
0.003424148	322.1468281
0.004408257	336.0680446
0.004986037	342.0420661
0.006146584	351.0880197

Table S1f. BET plot data for α-[Zn_4O(**L2**)$_3$]

BET Surface Area:	851.2808 ± 2.1324 m²/g
Slope:	0.005109 ± 0.000013 g/cm³ STP
Y-Intercept:	0.000005 ± 0.000000 g/cm³ STP
C:	1123.242801
Qm:	195.5529 cm³/g STP
Correlation Coefficient:	0.9999780
Molecular Cross-Sectional Area:	0.1620 nm²
Relative Pressure (p/p°)	**1/[Q(p°/p - 1)]**
0.00098701	9.22266E-06
0.007989658	4.56556E-05
0.009604812	5.38159E-05
0.010244691	5.70309E-05
0.01191498	6.54985E-05
0.014547726	7.88911E-05
0.015650236	8.44678E-05
0.018260705	9.77466E-05
0.0206576	0.000109923

Table S1g. BET plot data for α-[Zn_4O(**L1**)$_3$]⊃Cu

8. X-ray Diffraction Methods and Crystallographic Data for [Zn_4O(L1)$_3$] and α-[Zn_4O(L2)$_3$]

8.1 Single crystal X-ray crystallography

Crystals were mounted under oil on a plastic loop. X-ray diffraction data were collected with Mo-Kα radiation (λ = 0.7107 Å) using Oxford Diffraction X-calibur single crystal X-ray diffractometer at 150(2) K. Data sets were corrected for absorption using a multi-scan method, and structures were solved by direct methods using SHELXS-97[4] and refined by full-matrix least squares on F^2 by SHELXL-97,[5] interfaced through the program X-Seed.[6,7] In general, all non-hydrogen atoms were refined anisotropically and hydrogen atoms were included as invariants at geometrically estimated positions, unless specified otherwise in additional details below. Details of data collections and structure refinements are given below. CCDC-831356 and CCDC-831357 contains the supplementary crystallographic data for this structure. These data can be obtained free of charge from The Cambridge Crystallographic Data Centre via www.ccdc.cam.ac.uk/data_request/cif. A summary of the crystallographic data and structure refinements are given in Tables 1 and 2.

8.2 Additional refinement details

[Zn_4O(**L1**)$_3$]: The high angle data for the structure is weak. An ORTEP representation of the asymmetric unit of the structure is given in Figure 14. The phenyl ring is disordered over two positions corresponding to the racemic mixture of atropisomers that are observed in the solid-state. DFIX restraints (5) and one DELU command were used in the refinement to restrain the position of the phenol O atom (O8) and maintain chemically sensible C-C bond lengths and angles for the phenyl ring. EADP and EXYZ commands were used to allow a chemically sensible refinement of C6A/C6B. In the asymmetric unit Zn1 atom lies at a site with 3m symmetry, O1 is at a site with -4$_3$m symmetry, O2, C5 and C6A/C6B are at sites with m symmetry, and C3, C4 and C7 are at sites with mm symmetry. The structure has large solvent accessible voids. These contained a number of diffuse electron density peaks that could not be adequately identified and refined as solvent. The SQUEEZE routine of PLATON[5] was applied to the collected data, which resulted in significant reductions in R_1 and

wR_2 and an improvement in the GOF. R_1, wR_2 and GOF before SQUEEZE routine: 17.12%, 44.44% and 1.203; after SQUEEZE routine: 10.47%, 28.82% and 0.836. The contribution of disordered solvent (114 electrons/unit cell) equates to *ca.* two DEF solvent molecules which are included in the formula.

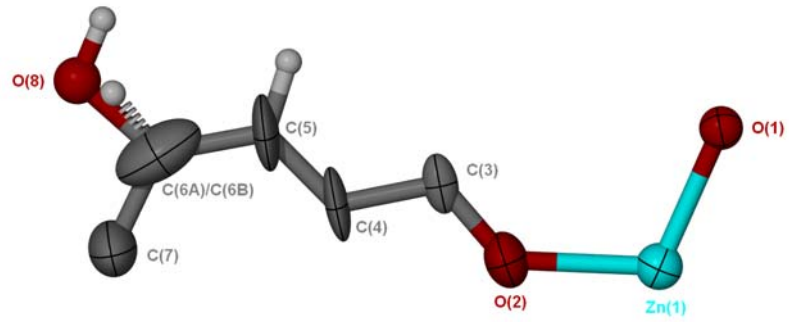

Figure 14. An ORTEP plot of the asymmetric unit of $[Zn_4O(\mathbf{L1})_3]$ with ellipsoids shown at the 50% probability level (O8 is shown as a sphere).

α-$[Zn_4O(\mathbf{L2})_3]$: The structure shows disorder of one of the methoxy groups (C8) and one of the phenyl rings and its attached methoxy group (C1' – C6' and O7'-C8'), the latter corresponding to the racemic mixture of atropisomers that are observed in the solid-state (Figure 15). The larger thermal ellipsoids for two carbon atoms (C2 and C3) in one of the phenyl rings indicate some disorder of that ring but this was not modelled. In the asymmetric unit Zn2 and O12 lie on a site with imposed 3m symmetry, while Zn1, C1 – C6, C9, O10, O11, O7, C1', C4' and C9' are at sites with m symmetry. The two largest peaks in the difference map are close to the Zn_4O cluster. The also structure has large solvent accessible voids and this was dealt with through the implementation of the SQUEEZE routine of PLATON.[5] In line with the treatment of $[Zn_4O(\mathbf{L1})_3]$, the SQUEEZE routine of PLATON was applied to the collected data, which resulted in reductions in R_1 and wR_2 and an improvement in the GOF. R_1, wR_2 and GOF before SQUEEZE routine: 5.98%, 18.27% and 1.613; after SQUEEZE routine: 4.76%, 12.79% and 1.121. The contribution of disordered solvent (28 electrons/unit cell) equates to approximately one DMF molecule per unit cell which was included in the formula.

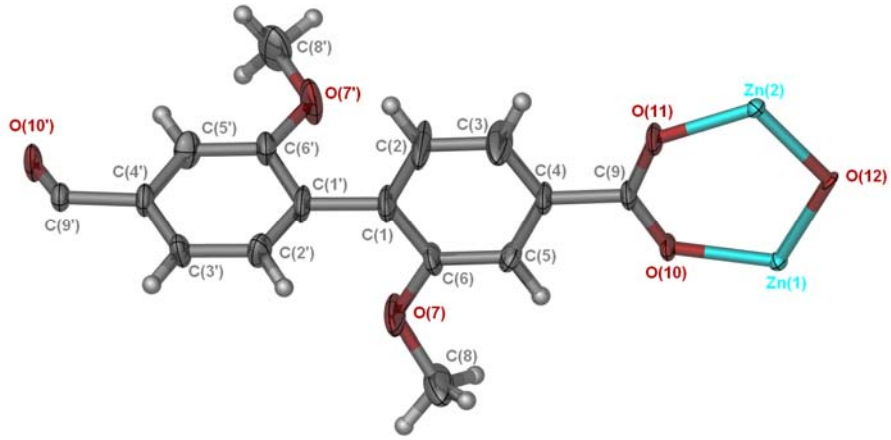

Figure 15. An ORTEP plot of the asymmetric unit of α-$[Zn_4O(\mathbf{L2})_3]$ with ellipsoids shown at the 50% probability level.

8.3 Powder X-ray Diffraction

Powder X-ray diffraction data was collected on a Rigaku Hiflux Homelab system using Cu-Kα radiation with an R-Axis IV++ image plate detector. Samples were mounted on plastic loops using paratone-N and data collected by scanning 90° in

phi for 120-300 second exposures. The data was converted into *xye* format using the program DataSqueeze. Simulated powder X-ray diffraction patterns were generated from the single crystal data using Mercury 2.3.

Table S2. Crystal data and structure refinement for $[Zn_4O(L1)_3]$.

Identification code	$[Zn_4O(\mathbf{L1})_3]$	
Empirical formula	$C_{52}H_{46}N_2O_{21}Zn_4$	
Formula weight	1094.09	
Temperature	150(2) K	
Wavelength	0.7107 Å	
Crystal system	Cubic	
Space group	*P*-4$_3$*m*	
Unit cell dimensions	a = 17.1227(14) Å	α= 90°.
	b = 17.1227(14) Å	β= 90°.
	c = 17.1227(14) Å	γ = 90°.
Volume	5020.2(7) Å^3	
Z	1	
Density (calculated)	0.429 Mg/m^3	
Absorption coefficient	0.494 mm^{-1}	
F(000)	660	
Crystal size	0.23 x 0.18 x 0.14 mm^3	
Theta range for data collection	2.66 to 28.13°.	
Index ranges	-10<=h<=21, -21<=k<=6, -11<=l<=15	
Reflections collected	4574	
Independent reflections	1870 [R(int) = 0.0898]	
Completeness to theta = 25.00°	99.6 %	
Absorption correction	Semi-empirical from equivalents	
Max. and min. transmission	1.00000 and 0.37536	
Refinement method	Full-matrix least-squares on F^2	
Data / restraints / parameters	1870 / 8 / 39	
Goodness-of-fit on F^2	0.832	
Final R indices [I>2sigma(I)]	R_1 = 0.1047, wR_2 = 0.2494	
R indices (all data)	R_1 = 0.1875, wR_2 = 0.2882	
Absolute structure parameter	0.19(9)	
Largest diff. peak and hole	0.572 and -0.617 e.Å^{-3}	

Table S3. Crystal data and structure refinement for α-[$Zn_4O(L2)_3$].

Identification code	α-[Zn_4O(**L2**)$_3$]	
Empirical formula	$C_{97}H_{72.33}N_{0.33}O_{38.33}Zn_8$	
Formula weight	2378.51	
Temperature	150(2) K	
Wavelength	0.7107 Å	
Crystal system	Rhombohedral	
Space group	*R*-3*m*	
Unit cell dimensions	a = 23.5302(8) Å	α= 90°.
	b = 23.5302(8) Å	β= 90°.
	c = 31.5110(14) Å	γ = 120°.
Volume	15109.3(10) $Å^3$	
Z	3	
Density (calculated)	0.784 Mg/m^3	
Absorption coefficient	0.979 mm^{-1}	
F(000)	3610	
Crystal size	0.42 x 0.34 x 0.22 mm^3	
Theta range for data collection	2.60 to 29.97°.	
Index ranges	-31<=h<=32, -31<=k<=32, -41<=l<=40	
Reflections collected	32081	
Independent reflections	4747 [R(int) = 0.0692]	
Completeness to theta = 27.00°	99.8 %	
Absorption correction	Semi-empirical from equivalents	
Max. and min. transmission	1.00000 and 0.88973	
Refinement method	Full-matrix least-squares on F^2	
Data / restraints / parameters	4747 / 0 / 168	
Goodness-of-fit on F^2	1.121	
Final R indices [I>2sigma(I)]	R_1 = 0.0476, wR_2 = 0.1197	
R indices (all data)	R_1 = 0.0735, wR_2 = 0.1279	
Largest diff. peak and hole	1.748 and -0.789 $e.Å^{-3}$	

9. References

(1) M. Rizzacasa, M. V. Sargent, *Aust. J. Chem.,* 1988, **41**, 1087.

(2) Brunauer, S.; Emmett, P. H.; Teller, E. *J. Am. Chem. Soc.* 1938, **60**, 309.

(3) K. S. Walton, R. Q. Snurr, *J. Am. Chem. Soc*., 2007, **129**, 8552-8556.

(4) G. M. Sheldrick, *Acta Cryst.* , 1990, **A46**, 467-.

(5) G. M. Sheldrick, *SHELXL-97*, University of Göttingen, Göttingen, Germany, 1997.

(6) L. J. Barbour, *J. Supramol. Chem.*, 2001, **1**, 189.

(7) A. L. Spek, *Acta Cryst.*, 1990, **A46**, C34.